

# Tunable deep-subwavelength superscattering using graphene monolayers

R. J. Li,<sup>1,2,3</sup> X. Lin,<sup>1,2,3</sup> S. S. Lin,<sup>1,2,3</sup> X. Liu,<sup>1</sup> and H. S. Chen<sup>1,2,3,\*</sup>

<sup>1</sup>State Key Laboratory of Modern Optical Instrumentation, Zhejiang University, Hangzhou 310027, China

<sup>2</sup>Department of Information Science and Electronic Engineering, Zhejiang University, Hangzhou 310027, China

<sup>3</sup>The Electromagnetics Academy of Zhejiang University, Zhejiang University, Hangzhou 310027, China

\*Corresponding author: hansomchen@zju.edu.cn

Compiled June 9, 2021

In this Letter, we theoretically propose for the first time that graphene monolayers can be used for superscatterer designs. We show that the scattering cross section of the bare deep-subwavelength dielectric cylinder is markedly enhanced by six orders of magnitude due to the excitation of the first-order resonance of graphene plamons. By utilizing the tunability of the plasmonic resonance through tuning graphene's chemical potential, the graphene superscatterer works in a wide range of frequencies from several terahertz to tens of terahertz. © 2021 Optical Society of America

OCIS codes: 310.6628, 290.4020, 240.3695, 240.0310.

Subwavelength structures can demonstrate very unusual electromagnetic properties with the concept of metamaterials [1]. The scattering of subwavelength structures can be suppressed to realize various devices, such as invisibility cloaks [2–7], but can be also enhanced to realize superscatterers, a kind of device that can magnify the scattering cross section of a given object remarkably [8] and that has potential applications ranging from detection, spectroscopy to photovoltaics [9–16].

Transformation optics and complementary metamaterials have been proposed to dramatically enhance the scattering cross section of a particle [8, 17, 18]. To implement this method, it requires both electrical and magnetic anisotropic inhomogeneous parameters. In order to loose the requirement, Ruan et al. [19, 20] and Mirzaei et al. [21, 22] use isotropic plasmonic structures to enhance the scattering cross sections. As the scattering cross sections of subwavelength structures experience the single channel limit [19, 23], they use multilayered plasmonic-dielectric structures to break the single channel limit by engineering an overlap of resonances of different plasmonic modes. However, when the sizes of subwavelength structures scale down to the deep-subwavelength, the scattering cross sections are extremely small and far below the single channel limit. The original structures in Refs. [19–22] can not be scaled down directly for superscattering purpose since the commonly available metals in nanophotonics have a thickness of several nanometers. This naturally raises the question of how to design a superscatterer which is suitable for the deep-subwavelength objects.

Graphene, a two dimensional hexagonal crystal carbon sheet with only one atom thick, can be a good candidate to solve this bottleneck. Since its ballistic transport and ultrahigh electron mobility, the surface conductivity of graphene is almost purely imaginary in the THz frequencies [24]. In other words, graphene can be treated as a thin film of metal with low loss. In the recent years,

graphene has attracted much attention as a good counterpart in the THz frequencies of metals in the optical frequencies, and the research area of graphene plasmonics has been flourished [25–32].

In this paper, we theoretically propose for the first time that graphene monolayers are used to design the superscatterer which can enlarge the scattering cross sections of deep-subwavelength dielectric objects in the THz frequencies. We introduce the model of superscatterer from Mie scattering theory. With the graphene monolayer, the scattering cross section can be enhanced by six orders of magnitude. The applicability for dielectric media with different permittivities and different incident frequencies are analysed by utilizing the tunability of surface conductivity of graphene.

As shown in Fig. 1, the case of a TM-polarized plane wave with magnitude  $H_0$  normally incidents from air onto an infinite long graphene coated cylindrical dielectric medium is considered. The incident magnetic field is  $\mathbf{H} = H_0 e^{ik_0 x} \hat{z}$  with the time dependence of  $\exp(-i\omega t)$ , where  $k_0 = \omega \sqrt{\varepsilon_0 \mu_0}$  is the wavenumber in free space and  $\omega$  is the angular frequency of the incident field. The radius of the dielectric medium is  $R$ . The relative permittivity of the dielectric medium is  $\varepsilon_r$ , and the relative permeability is  $\mu_r = 1$ .

Since graphene is a two dimensional electromagnetic material and its thickness is extremely small compared with the radius of the cylindrical dielectric medium, we will treat it as a conducting film with surface conductivity  $\sigma_g$  [24, 33]. From Mie scattering theory, the magnetic field can be written as  $H_z = H_0 \sum_{n=0}^{\infty} a_n [J_n(k_0 r) + s_n H_n^{(1)}(k_0 r)] \cos(n\theta)$  for  $r > R$ , and  $H_z = H_0 \sum_{n=0}^{\infty} b_n J_n(kr) \cos(n\theta)$  for  $r \leq R$ , where  $a_n = \delta_n i^n$  ( $\delta_n = 1$  for  $n = 0$  and  $\delta_n = 2$  for  $n \neq 0$ ),  $k = k_0 \sqrt{\varepsilon_r}$  is the wavenumber in dielectric medium,  $s_n$  is the scattering coefficient,  $J_n$  and  $H_n^{(1)}$  are the  $n$ -th order Bessel function of the first kind and Hankel function of

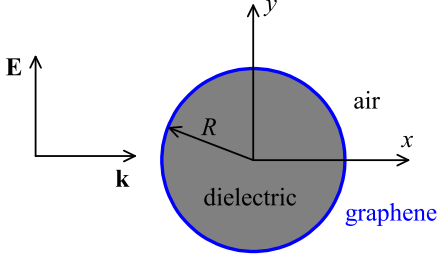


Fig. 1. Cross-sectional view of the superscatterer. The cylindrical dielectric medium (grey area) is coated with the graphene monolayer (blue area). A TM-polarized plane wave with magnitude  $H_0$  normally incidents onto the superscatterer. The radius of the dielectric medium is  $R$ .

the first kind, respectively [34]. According to the continuity conditions at  $r = R$ , the scattering coefficient can be obtained as

$$s_n = -\frac{J'_n(k_0 R) t_n - J_n(k_0 R) J'_n(kR)}{H_n^{(1)'}(k_0 R) t_n - H_n^{(1)}(k_0 R) J'_n(kR)}, \quad (1)$$

where  $t_n = \sqrt{\varepsilon_r} J_n(kR) + i\sigma_g \eta_0 J'_n(kR)$ ,  $\sigma_g$  is the surface conductivity of graphene,  $\eta_0 = \sqrt{\mu_0/\varepsilon_0}$  is the impedance of free space. We define the normalized scattering cross section (NSCS) as  $\text{NSCS} = \sum_{n=0}^{\infty} \delta_n |s_n|^2$ , which is normalized by  $2\lambda/\pi$  and we have considered the degeneracy between  $|s_n|$  and  $|s_{-n}|$  [22]. Note when  $\sigma_g = 0$ , it reduces to the case of scattering by a bare cylindrical dielectric medium.

The surface conductivity of graphene can be calculated according to the Kubo formula  $\sigma_g(\omega, \mu_c, \Gamma, T) = \sigma_{intra} + \sigma_{inter}$ , where

$$\sigma_{intra} = \frac{ie^2 k_B T}{\pi \hbar^2 (\omega + i2\Gamma)} \left[ \frac{\mu_c}{k_B T} + 2 \ln \left( e^{-\mu_c/k_B T} + 1 \right) \right] \quad (2)$$

is due to intraband contribution, and

$$\sigma_{inter} = \frac{ie^2 (\omega + i2\Gamma)}{\pi \hbar^2} \int_0^\infty \frac{f_d(-\varepsilon) - f_d(\varepsilon)}{(\omega + i2\Gamma)^2 - 4(\varepsilon/\hbar)^2} d\varepsilon \quad (3)$$

is due to interband contribution [33, 35]. In the above formula,  $-e$  is the charge of an electron,  $\hbar = h/2\pi$  is the reduced Plank's constant,  $\omega = 2\pi f$  is the angular frequency of the incident field,  $\Gamma$  is the phenomenological scattering rate that is assumed to be independent of the energy  $\varepsilon$ ,  $f_d(\varepsilon) = 1/(e^{(\varepsilon - \mu_c)/k_B T} + 1)$  is the Fermi-Dirac distribution,  $k_B$  is the Boltzmann's constant,  $T$  is the temperature, and  $\mu_c$  is the chemical potential which can be tuned by a gate voltage and/or chemical doping. In the following, we choose  $\Gamma = 0.11$  meV,  $T = 300$  K and the chemical potential  $\mu_c$  is tuned between 0 eV to 0.5 eV [33]. Thus, for a given frequency and chemical potential we can obtain the surface conductivity of graphene and calculate the NSCS of the superscatterer for a given inside dielectric medium. As an example, we let  $\varepsilon_r = 1.44$ ,  $f = 15$  THz and

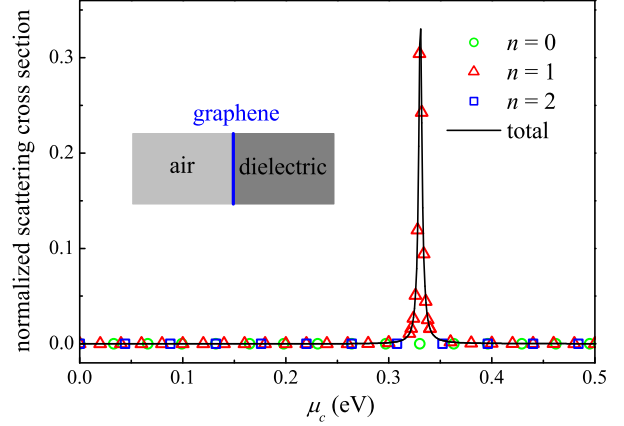


Fig. 2. Schematically shows the total normalized scattering cross section (NSCS) and the contributions of the first three scattering terms as a function of the chemical potential  $\mu_c$ . The inset shows the equivalent planar structure. The parameters are  $\varepsilon_r = 1.44$ ,  $f = 15$  THz and  $R = 0.2 \mu\text{m}$ .

$R = 0.2 \mu\text{m}$ . Under these parameters, this structure corresponds to a graphene coated deep-subwavelength dielectric cylinder. Fig. 2 schematically shows the dependence between NSCS and the chemical potential  $\mu_c$  which exhibits a sharp resonance. The superscattering occurs at  $\mu_c = 0.331$  eV with the maximum NSCS equals to 0.343. For comparison, we also plot the contributions of the first three scattering terms in the figure. Clearly, the resonance of NSCS is caused by the resonance of the first order scattering term ( $n = 1$ ). To validate this, we use the series forms of Bessel function and Hankel function to simplify the scattering coefficient  $s_n$  [36]. For a deep-subwavelength dielectric cylinder which satisfies  $kR \ll 1$ , only the first orders of the series are needed. Detailed calculations show

$$s_1 = \frac{i\pi k_0^2 R^2 (\varepsilon - 1) k_0 R + i\sigma_g \eta_0}{4 (\varepsilon + 1) k_0 R + i\sigma_g \eta_0}, \quad (4)$$

which exhibits a resonance at  $\sigma_g = i(\varepsilon + 1) k_0 R/\eta_0 = 0.407i$  mS when the graphene is assumed to be lossless. It is approximately equal to the result from Mie scattering theory where  $\sigma_g = 0.001 + 0.409i$  mS. Since the real part of conductivity is small compared with its imaginary part, this superscatterer has a large scattering cross section with low energy dissipation. Note when there is no graphene, the NSCS of the dielectric medium is  $6.254 \times 10^{-7}$ . This indicates that coating with the properly doped and/or gated graphene monolayer can greatly enhance the scattering by six orders of magnitude. Although this kind of superscatterer is realized by only one resonant mode which still experiences the single channel limit and it is different to Refs. [19–22], the scattering cross section has enlarged significantly which is enough to demonstrate the superscattering phenomenon.

There are two critical conditions to realize this kind of superscattering: permittivity and optical loss, which cor-

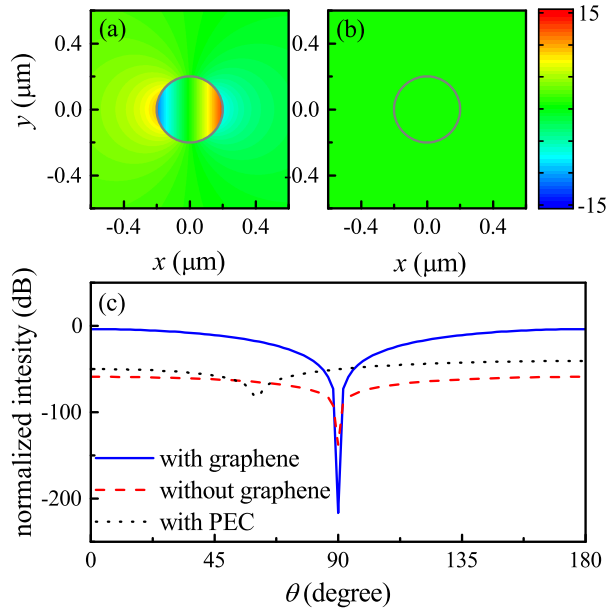


Fig. 3. Top panel: normalized magnetic field distributions for (a) dielectric medium coated with the graphene monolayer and (b) the bare dielectric medium. Bottom panel: far field scattering patterns for the dielectric medium coated with graphene (blue solid line), without graphene (red dashed line) and with PEC (black dotted line), respectively. The grey circles in (a) and (b) indicate the boundary of the dielectric cylinder. The parameters are  $\epsilon_r = 1.44$ ,  $f = 15$  THz,  $R = 0.2 \mu\text{m}$  and  $\mu_c = 0.331$  eV.

respond to the imaginary part and real part of the surface conductivity, respectively. The permittivity of the coating layer must be delicately determined to satisfy the resonant condition [19,37]. The inset in Fig. 2 shows the equivalent planar structure, and its corresponding dispersion relation of the graphene plasmon is

$$\left(1 + i \frac{\sigma_g k_1}{\omega \epsilon_0 \epsilon_r}\right) k_2 + \frac{k_1}{\epsilon_r} = 0, \quad (5)$$

where  $k_1 = (\beta^2 - k_0^2 \epsilon_r)^{1/2}$ ,  $k_2 = (\beta^2 - k_0^2)^{1/2}$ , and  $\beta$  is the propagation constant. For parameters in Fig. 2 and assuming that the graphene is lossless, the propagation constant is  $\beta = 15.878 k_0$  at  $\mu_c = 0.331$  eV which is nearly equal to the first order Bohr condition  $\beta = 50/\pi k_0$  [37]. Meanwhile, the optical loss of the coating layer should be small enough. Actually, if we increase the real part of surface conductivity of graphene by 10 times, i.e.  $\sigma_g = 0.010 + 0.409i$  mS, the corresponding NSCS at the resonant point  $\mu_c = 0.331$  eV would be 0.008 which is only 2.5% of the original value. Moreover, the thickness of graphene is small compared with the radius of the deep-subwavelength dielectric cylinder. Thus graphene is indeed a good choice for the study of super-scattering of deep-subwavelength dielectric objects and the design of corresponding superscatterers.

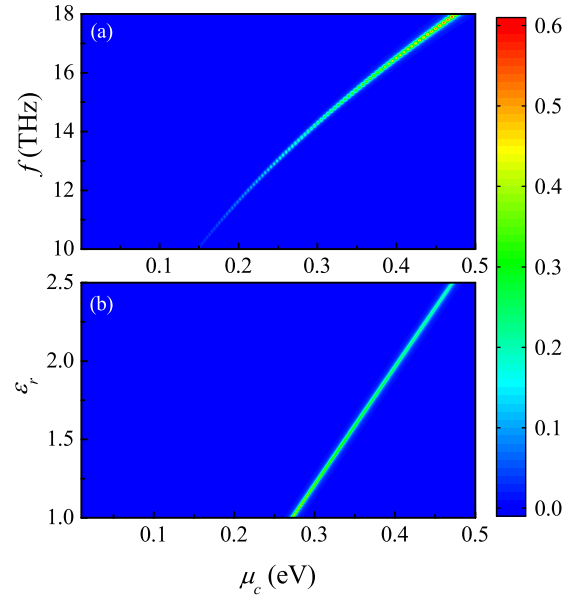


Fig. 4. The normalized scattering cross sections (NSCSs) for (a) different incident frequencies and (b) dielectric media with different permittivities when the chemical potential  $\mu_c$  is tuned between 0 eV to 0.5 eV, respectively. The parameters are  $\Gamma = 0.11$  meV,  $T = 300$  K,  $R = 0.2 \mu\text{m}$  for both (a) and (b), while  $\epsilon_r = 1.44$  for (a), and  $f = 15$  THz for (b).

Fig. 3 schematically shows the normalized magnetic field distributions and far field scattering patterns. When the dielectric medium is coated with the graphene monolayer with  $\mu_c = 0.331$  eV, the normalized magnetic field intensity at the center of the medium is almost zero and the scattering is enhanced both in the forward direction and the backward direction (See Fig. 3 (a)). Whereas, when the graphene is removed, the corresponding magnetic field is almost unperturbed as shown in Fig. 3 (b)-(c). Note although zero field intensity inside the dielectric cylinder can also be realized just by coating the dielectric medium with a PEC, however, as shown in Fig. 3 (c), the far field scattering patterns of graphene coated dielectric medium and PEC coated dielectric medium are totally different. This can be understood by calculating the equivalent relative permittivity of graphene.

Under our optimized parameters, the permittivity of graphene is  $\epsilon_g = -489.4 + 1.8i$  which is calculated by the formula  $\epsilon_g = 1 + i\sigma_g/\omega\epsilon_0 d$ , where  $d$  is the thickness of graphene. In the calculation, we let  $d = 1$  nm which is commonly used in the simulation of graphene plasmonics [24]. Thus graphene can be treated as a thin film of low loss metal. Whereas, the PEC is a kind of metal with infinite loss. In fact, calculations show that the NSCS of PEC coated dielectric medium is  $2.883 \times 10^{-5}$ . This indicates that our result is not the trivial outcome with the use of negative permittivity materials.

In practical applications, the tunability of a device

is of great importance. Since the chemical potential of graphene can be tuned by a gate voltage and/or chemical doping, this provides a versatile method to manipulate the superscattering of deep-subwavelength dielectric objects. To this end, we vary the frequency of incident wave and the permittivity of dielectric medium, respectively, and calculate the corresponding NSCS when the chemical potential  $\mu_c$  is tuned between 0 eV to 0.5 eV. For simplicity, the dispersion of the dielectric medium is neglected. As shown in Fig. 4(a), the superscattering occurs between  $f = 10$  THz to  $f = 18$  THz with relative large values of NSCSs, which indicates that we can tune the chemical potential of graphene delicately to get the superscattering phenomenon. Although the maximum NSCS at lower frequencies is less than 0.04, it is still much larger than the NSCS of the bare dielectric medium. Similarly, the superscattering also occurs when the relative permittivity varies between  $\varepsilon_r = 1$  to  $\varepsilon_r = 2.5$  and their corresponding NSCSs have relative large values as shown in Fig. 4(b). This indicates that this superscatterer is suitable for dielectric media with low permittivities.

In conclusion, we demonstrate the possibility of superscattering of deep-subwavelength dielectric objects by graphene monolayers. The resonance of the first order scattering term can be emerged by tuning the chemical potential of graphene. This superscatterer is applicable in a wide range of frequencies from several terahertz to tens of terahertz and it is suitable for the superscattering of dielectric media with low permittivities. This superscattering effect may be useful in practical THz devices such as detectors and sensors.

This work was sponsored by the National Natural Science Foundation of China under Grants No. 61322501, and No. 61275183, the National Program for Special Support of Top-Notch Young Professionals, the Program for New Century Excellent Talents (NCET-12-0489) in University, and the Fundamental Research Funds for the Central Universities (2014XZZX003-24).

## References

1. N. Zheludev and Y. Kivshar, *Nat. Mater.* **11**, 917 (2012).
2. A. Alù and N. Engheta, *Phys. Rev. E* **72**, 016623 (2005).
3. B. Edwards, A. Alù, M. G. Silveirinha, and N. Engheta, *Phys. Rev. Lett.* **103**, 153901 (2009).
4. A. Alù and N. Engheta, *Phys. Rev. Lett.* **102**, 233901 (2009).
5. P. Y. Chen, J. Soric, and A. Alù, *Adv. Mater.* **24**, OP281 (2012).
6. P. Y. Chen and A. Alù, *ACS Nano* **5**, 5855 (2011).
7. S. Xu, Y. Wang, B. Zhang, H. Chen, *SCIENCE CHINA Information Sciences* **56**, 120408 (2013).
8. T. Yang, H. Chen, X. Luo, and H. Ma, *Opt. Exp.* **16**, 18545 (2008).
9. S. Nie and S. R. Emory, *Science* **275**, 1102 (1997).
10. J. B. Jackson and N. J. Halas, *Proc. Natl. Acad. Sci. U.S.A.* **101**, 17930 (2004).
11. R. Bardhan, S. Mukherjee, N. A. Mirin, S. D. Levit, P. Nordlander, and N. J. Halas, *J. Phys. Chem. C* **114**, 7378 (2010).
12. H. R. Stuart and D. G. Hall, *Appl. Phys. Lett.* **73**, 3815 (1998).
13. F. Hao, Y. Sonnefraud, P. V. Dorpe, S. A. Maier, N. J. Halas, and P. Nordlander, *Nano Lett.* **8**, 3983 (2008).
14. J. Aizpurua, P. Hanarp, D. S. Sutherland, M. Käll, G. W. Bryant, and F. J. Garcia de Abajo, *Phys. Rev. Lett.* **90**, 057401 (2003).
15. S. Pillai, K. R. Catchpole, T. Trupke, and M. A. Green, *J. Appl. Phys.* **101**, 093105 (2007).
16. H. A. Atwater and A. Polman, *Nat. Mater.* **9**, 205 (2010).
17. W. H. Wee and J. B. Pendry, *New J. Phys.* **11**, 073033 (2009).
18. W. Jiang, B. Xu, Q. Cheng, T. Cui, and G. Yu, *J. Opt. Soc. Am. A* **30**, 1698 (2013).
19. Z. Ruan and S. Fan, *Phys. Rev. Lett.* **105**, 013901 (2010).
20. Z. Ruan and S. Fan, *Appl. Phys. Lett.* **98**, 043101 (2011).
21. A. Mirzaei, I. V. Shadrivov, A. E. Miroshnichenko, and Y. S. Kivshar, *Opt. Exp.* **21**, 10454 (2014).
22. A. Mirzaei, A. E. Miroshnichenko, I. V. Shadrivov, and Y. S. Kivshar, *Appl. Phys. Lett.* **105**, 011109 (2014).
23. M. I. Tribelsky and B. S. Luk'yanchuk, *Phys. Rev. Lett.* **97**, 263902 (2006).
24. A. Vakil and N. Engheta, *Science* **332**, 1291 (2011).
25. P. R. West, S. Ishii, G. V. Naik, N. K. Emani, V. M. Shalaev, and A. Boltasseva, *Laser Photonics Rev.* **4**, 795 (2010).
26. F. Bonaccorso, Z. Sun, T. Hasan, and A. C. Ferrari, *Nat. Photon.* **4**, 611 (2010).
27. A. N. Grigorenko, M. Polini, and K. S. Novoselov, *Nat. Photon.* **6**, 749 (2012).
28. A. Marini, D. V. Skryabin, and B. Malomed, *Opt. Exp.* **19**, 6616 (2011).
29. Y. V. Bludov, D. A. Smirnova, Y. S. Kivshar, N. M. R. Peres, and M. I. Vasilevskiy, *Phys. Rev. B* **89**, 035406 (2014).
30. M. L. Nesterov, J. B. Abad, A. Yu. Nikitin, F. J. G. Vidal, and L. M. Moreno, *Laser Photon. Rev.* **7**, L7 (2013).
31. D. A. Smirnova, I. V. Shadrivov, A. I. Smirnov, and Y. S. Kivshar, *Laser Photon. Rev.* **8**, 291 (2014).
32. C. Huang, F. Ye, Z. Sun, and X. Chen, *Opt. Exp.* **22**, 30108 (2014).
33. G. W. Hanson, *J. Appl. Phys.* **103**, 064302 (2008).
34. C. F. Bohren and D. R. Huffman, *Absorption and Scattering of Light by Small Particles* (Wiley, New York, 1983).
35. V. P. Gusynin, S. G. Sharapov, and J. P. Carbotte, *J. Phys.: Condens. Matter* **19**, 026222 (2007).
36. M. Abramowitz and I. A. Stegun, *Handbook of Mathematical Functions with Formulas, Graphs, and Mathematical Tables* (Dover, New York, 1965).
37. W. Liu, R. F. Oulton, and Y. S. Kivshar, Preprint at <http://arxiv.org/abs/1412.3929> (2014).

## Informational Fifth Page

In this section, please provide full versions of citations to assist reviewers and editors (OL publishes a short form of citations) or any other information that would aid the peer-review process.

## References

1. N. Zheludev and Y. Kivshar, "From metamaterials to metadevices," *Nat. Mater.* **11**, 917 (2012).
2. A. Alù and N. Engheta, "Achieving transparency with plasmonic and metamaterial coatings," *Phys. Rev. E* **72**, 016623 (2005).
3. B. Edwards, A. Alù, M. G. Silveirinha, and N. Engheta, "Experimental Verification of Plasmonic Cloaking at Microwave Frequencies with Metamaterials," *Phys. Rev. Lett.* **103**, 153901 (2009).
4. A. Alù and N. Engheta, "Cloaking a Sensor," *Phys. Rev. Lett.* **102**, 233901 (2009).
5. P. Y. Chen, J. Soric, and A. Alù, "Invisibility and Cloaking Based on Scattering Cancellation," *Adv. Mater.* **24**, OP281 (2012).
6. P. Y. Chen and A. Alù, "Atomically Thin Surface Cloak Using Graphene Monolayers," *ACS Nano* **5**, 5855 (2011).
7. S. Xu, Y. Wang, B. Zhang, H. Chen, "Invisibility cloaks from forward design to inverse design," *SCIENCE CHINA Information Sciences* **56**, 120408 (2013).
8. T. Yang, H. Chen, X. Luo, and H. Ma, "Superscatterer: Enhancement of scattering with complementary media," *Opt. Exp.* **16**, 18545 (2008).
9. S. Nie and S. R. Emory, "Probing Single Molecules and Single Nanoparticles by Surface-Enhanced Raman Scattering," *Science* **275**, 1102 (1997).
10. J. B. Jackson and N. J. Halas, "Surface-enhanced Raman scattering on tunable plasmonic nanoparticle substrates," *Proc. Natl. Acad. Sci. U.S.A.* **101**, 17930 (2004).
11. R. Bardhan, S. Mukherjee, N. A. Mirin, S. D. Levit, P. Nordlander, and N. J. Halas, "Nanosphere-in-a-Nanoshell: A Simple Nanomatryushka," *J. Phys. Chem. C* **114**, 7378 (2010).
12. H. R. Stuart and D. G. Hall, "Island size effects in nanoparticle-enhanced photodetectors," *Appl. Phys. Lett.* **73**, 3815 (1998).
13. F. Hao, Y. Sonnefraud, P. V. Dorpe, S. A. Maier, N. J. Halas, and P. Nordlander, "Symmetry Breaking in Plasmonic Nanocavities: Subradiant LSPR Sensing and a Tunable Fano Resonance," *Nano Lett.* **8**, 3983 (2008).
14. J. Aizpurua, P. Hanarp, D. S. Sutherland, M. Käll, G. W. Bryant, and F. J. Garcia de Abajo, "Optical Properties of Gold Nanorings," *Phys. Rev. Lett.* **90**, 057401 (2003).
15. S. Pillai, K. R. Catchpole, T. Trupke, and M. A. Green, "Surface plasmon enhanced silicon solar cells," *J. Appl. Phys.* **101**, 093105 (2007).
16. H. A. Atwater and A. Polman, "Plasmonics for improved photovoltaic devices," *Nat. Mater.* **9**, 205 (2010).
17. W. H. Wee and J. B. Pendry, "Shrinking optical devices," *New J. Phys.* **11**, 073033 (2009).
18. W. Jiang, B. Xu, Q. Cheng, T. Cui, and G. Yu, "Design and rigorous analysis of transformation-optics scaling devices," *J. Opt. Soc. Am. A* **30**, 1698 (2013).
19. Z. Ruan and S. Fan, "Superscattering of Light from Subwavelength Nanostructures," *Phys. Rev. Lett.* **105**, 013901 (2010).
20. Z. Ruan and S. Fan, "Design of subwavelength superscattering nanospheres," *Appl. Phys. Lett.* **98**, 043101 (2011).
21. A. Mirzaei, I. V. Shadrivov, A. E. Miroshnichenko, and Y. S. Kivshar, "Cloaking and enhanced scattering of core-shell plasmonic nanowires," *Opt. Exp.* **21**, 10454 (2014).
22. A. Mirzaei, A. E. Miroshnichenko, I. V. Shadrivov, and Y. S. Kivshar, "Superscattering of light optimized by a genetic algorithm," *Appl. Phys. Lett.* **105**, 011109 (2014).
23. M. I. Tribelsky and B. S. Luk'yanchuk, "Anomalous Light Scattering by Small Particles," *Phys. Rev. Lett.* **97**, 263902 (2006).
24. A. Vakil and N. Engheta, "Transformation Optics Using Graphene," *Science* **332**, 1291 (2011).
25. P. R. West, S. Ishii, G. V. Naik, N. K. Emani, V. M. Shalvaev, and A. Boltasseva, "Searching for better plasmonic materials," *Laser Photonics Rev.* **4**, 795 (2010).
26. F. Bonaccorso, Z. Sun, T. Hasan, and A. C. Ferrari, "Graphene photonics and optoelectronics," *Nat. Photon.* **4**, 611 (2010).
27. A. N. Grigorenko, M. Polini, and K. S. Novoselov, "Graphene plasmonics," *Nat. Photon.* **6**, 749 (2012).
28. A. Marini, D. V. Skryabin, and B. Malomed, "Stable spatial plasmon solitons in a dielectric-metal-dielectric geometry with gain and loss," *Opt. Exp.* **19**, 6616 (2011).
29. Y. V. Bludov, D. A. Smirnova, Y. S. Kivshar, N. M. R. Peres, and M. I. Vasilevskiy, "Nonlinear TE-polarized surface polaritons on graphene," *Phys. Rev. B* **89**, 035406 (2014).
30. M. L. Nesterov, J. B. Abad, A. Yu. Nikitin, F. J. G. Vidal, and L. M. Moreno, "Graphene supports the propagation of subwavelength optical solitons," *Laser Photon. Rev.* **7**, L7 (2013).
31. D. A. Smirnova, I. V. Shadrivov, A. I. Smirnov, and Y. S. Kivshar, "Dissipative plasmon-solitons in multilayer graphene," *Laser Photon. Rev.* **8**, 291 (2014).
32. C. Huang, F. Ye, Z. Sun, and X. Chen, "Tunable subwavelength photonic lattices and solitons in periodically patterned graphene monolayer," *Opt. Exp.* **22**, 30108 (2014).
33. G. W. Hanson, "Dyadic Greens functions and guided surface waves for a surface conductivity model of graphene," *J. Appl. Phys.* **103**, 064302 (2008).
34. C. F. Bohren and D. R. Huffman, *Absorption and Scattering of Light by Small Particles* (Wiley, New York, 1983).
35. V. P. Gusynin, S. G. Sharapov, and J. P. Carbotte, "Magneto-optical conductivity in graphene," *J. Phys.: Condens. Matter* **19**, 026222 (2007).
36. M. Abramowitz and I. A. Stegun, *Handbook of Mathematical Functions with Formulas, Graphs, and Mathematical Tables* (Dover, New York, 1965).
37. W. Liu, R. F. Oulton, and Y. S. Kivshar, "Geometric interpretations for resonances of plasmonic nanoparticles," Preprint at <http://arxiv.org/abs/1412.3929> (2014).